



Snow accumulation variability derived from radar and firn core data along a 600 km transect in Adelie Land, East Antarctic plateau

D. Verfaillie, M. Fily, E. Le Meur, O. Magand, B. Jourdain, L. Arnaud, and V. Favier

Laboratoire de Glaciologie et Géophysique de l'Environnement, UMR5183, Saint-Martin-d'Hères, France

Correspondence to: D. Verfaillie (dverfaillie@lgge.obs.ujf-grenoble.fr)

Received: 12 June 2012 – Published in The Cryosphere Discuss.: 24 July 2012

Revised: 25 October 2012 – Accepted: 26 October 2012 – Published: 16 November 2012

Abstract. The mass balance of ice sheets is an intensively studied topic in the context of global change and sea-level rise. However – particularly in Antarctica – obtaining mass balance estimates remains difficult due to various logistical problems. In the framework of the TASTE-IDEA (Trans-Antarctic Scientific Traverses Expeditions – Ice Divide of East Antarctica) program, an International Polar Year project, continuous ground penetrating radar (GPR) measurements were carried out during a traverse in Adelie Land (East Antarctica) during the 2008–2009 austral summer between the Italian–French Dome C (DC) polar plateau site and French Dumont D'Urville (DdU) coastal station. The aim of this study was to process and interpret GPR data in terms of snow accumulation, to analyse its spatial and temporal variability and compare it with historical data and modelling. The focus was on the last 300 yr, from the pre-industrial period to recent times. Beta-radioactivity counting and gamma spectrometry were applied to cores at the LGGE laboratory, providing a depth–age calibration for radar measurements. Over the 600 km of usable GPR data, depth and snow accumulation were determined with the help of three distinct layers visible on the radargrams (≈ 1730 , 1799 and 1941 AD). Preliminary results reveal a gradual increase in accumulation towards the coast (from ≈ 3 cm w.e. a^{-1} at Dome C to ≈ 17 cm w.e. a^{-1} at the end of the transect) and previously undocumented undulating structures between 300 and 600 km from DC. Results agree fairly well with data from previous studies and modelling. Drawing final conclusions on temporal variations is difficult because of the margin of error introduced by density estimation. This study should have various applications, including model validation.

1 Introduction

Polar regions play a significant role in the climate system. Large ice sheets located over Greenland and Antarctica influence the water cycle and thermohaline circulation through the capture or release of freshwater. These regions also are crucial for Earth radiation budget due to high snow and ice albedos. Hence, in the context of global climate change (Solomon et al., 2007), particular attention is being paid to the mass balance of Polar ice sheets.

In order to predict the behaviour of ice sheets under future climate conditions (i.e. their contribution to future sea-level rise), it is necessary (1) to assess their past and current state and (2) to understand the physical processes linking climate to the ice sheet mass balance. To this end, ice cores provide precious information on quaternary climate and atmospheric composition. However, obtaining the accurate Antarctic mass balance remains difficult, but can mainly be achieved through field measurements, which are generally interpolated by the use of remote sensing data. The resulting SMB maps are used to validate model outputs. Mass balance is the algebraic sum of two terms: the accumulation of snow on the surface of the ice sheet (through precipitation, hoar formation and wind deposition), which can be complemented by some refreezing at its base; and its ablation (through sublimation, surface and basal melting, wind scouring and iceberg calving). Surface mass balance (SMB) only refers to processes occurring at the surface of the ice sheet.

However, in Antarctica SMB remains poorly known. Its high variability and the shortness of the studied time periods make the observation of SMB trends difficult. Trends often appear inexistent, which seems to be the case for example in the coastal part of Adelie Land (Agosta et al., 2011). Another

example is the slight increase in surface elevation that has been observed in the interior of the continent, suggesting a recent gain in mass (e.g. Helsen et al., 2008), whereas precipitation appears not to have undergone any significant change since the 1950s (Monaghan et al., 2006a). This contradiction highlights the uncertainty of SMB measurements and interpretations, which result in a high level of uncertainty concerning the future contribution of Antarctic SMB to sea level rise (Meehl et al., 2007).

Various ground-based techniques are used to determine SMB in Antarctica, such as stake farms or lines, ultrasonic sensors, snow pits and firn/ice cores (Eisen et al., 2008). Density is an important parameter which has to be known accurately, as well as the depth vs. age relationship. The latter can be determined by layer counting, radiochronology (decay of natural radioactive isotopes such as ^{210}Pb) or the determination of reference horizons (volcanic layers or radioactive horizons resulting from the atmospheric nuclear weapon tests carried out between the 1950s and the 1980s) (Eisen et al., 2008; Magand, 2009).

However, all these methods yield localised data and thus suffer from poor spatial representativeness. On the other hand, ground penetrating radar (GPR), offers the possibility to determine accumulation continuously over several hundreds of kilometres. GPR has been used previously in specific areas in East Antarctica, among others in Dronning Maud Land (e.g. Richardson et al., 1997; Richardson and Holmlund, 1999), along the Norwegian–US scientific traverse (Muller et al., 2010), or close to South Pole Station (Arcone et al., 2005a), providing precious information on snow accumulation in these areas. It is thus a powerful tool to assess its spatial (and temporal) variability and can be used to link firn/ice cores and stakes SMB measurements. However, such GPR studies are sparse and large regions in East Antarctica – especially in the interior of the continent – remain uncovered.

The aim of the present study was thus to improve our knowledge of East-Antarctic SMB by analysing new data (radar and firn cores) obtained along a transect between the Italian–French Concordia Dome C polar station (DC) and the French Dumont-Durville station (DdU) (Fig. 1). This round-trip traverse was made from 20 January to 10 February 2009 as part of the ANR-VANISH (Vulnerability of the ANtarctic Ice-Sheet) and IPEV-TASTE-IDEA (Trans-Antarctic Scientific Traverses Expeditions – Ice Divide of East Antarctica) scientific programs. During this traverse, (nearly) continuous radar measurements were made and 6 firn cores (16.5 to 21 m deep) were drilled (Fig. 1). Beta-radioactivity measurements and gamma spectrometry analysis of the cores at LGGE laboratory (Laboratoire de Glaciologie et Géophysique de l'Environnement) provided a depth–age calibration for radar measurements.

This transect is among the most documented ones in East Antarctica and has been followed regularly and studied since the 1970s (see for example the works of Pourchet et al., 1983;

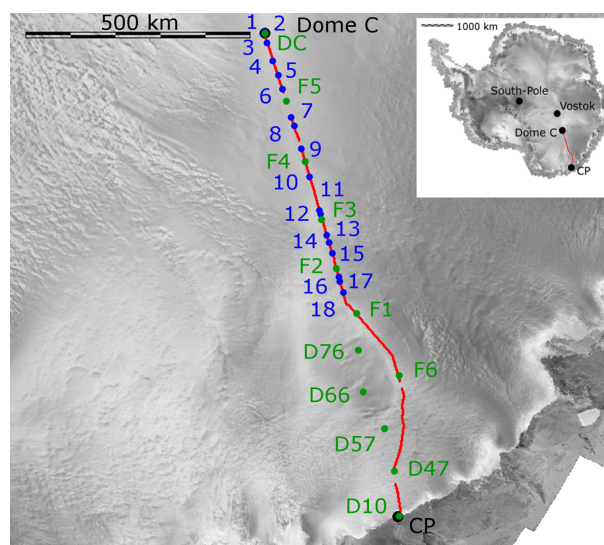


Fig. 1. Map of Antarctica showing the location of the radar section analysed (numbered 1 to 18, in blue) and cores (in green). Each blue number corresponds to the beginning of a radargram. A general map of Antarctica is inserted in the top right corner to show the location of the main scientific stations on the Antarctic plateau and East Antarctica, as well as the transect between DC and Dumont-d'Urville (Cap Prud'Homme is indicated on the map instead of Dumont-d'Urville, the latter being located on an island 5 km offshore).

Pettré et al., 1986). However, the data in this region are not evenly distributed. SMB measurements have been carried out regularly in the coastal area since 2004 (Genthon et al., 2007; Agosta et al., 2011; Favier et al., 2011). Other studies focused on the DC sector (Petit et al., 1982; Urbini et al., 2008). Frezzotti et al. (2004, 2005) used snow radar as well as stake farms, ice cores, surface morphology and remote sensing to estimate spatial and temporal variability of the SMB along a transect from Terra Nova Bay to DC, and from D66 to Talos Dome (Magand et al., 2004). However, SMB measurements between DC and the coast are sparse and no SMB radar measurements had ever been made along the DC–DdU traverse.

In the current study, the radar data was processed and interpreted in terms of SMB to analyse its spatial and temporal variability along the DC–DdU traverse. Results were compared with historical data in the region (Pettré et al., 1986; Mulvaney and Wolff, 1994; Pourchet et al., 2003; Frezzotti et al., 2004; Urbini et al., 2008) and to four SMB climatologies (Arthern et al., 2006; van de Berg et al., 2006, ERA-Interim and LMDZ4). We focused on the pre-industrial to the industrial period, which spans the last 300 yr (approximately the top 70 m of snow, or the first 750 ns of the radargrams).

Section 2 deals with the available radar and firn core data and the various methods used in this study. The results are subsequently displayed in Sect. 3, and discussed in Sect. 4.

2 Data and methods

2.1 Radar

Ground penetrating radar (GPR), also referred to as ice-penetrating radar, snow radar or radio echo sounding, is widely used in different fields, including engineering, archeology, seismic exploration, glaciology. It is used for mapping the internal structures of a substrate, or locating objects in cases of archeology and construction engineering (Daniels, 2000; Eisen et al., 2008). The main advantage of this method is that it provides a continuous measurement, in contrast with other widely used glaciological SMB measurements such as stakes or firn/ice cores. However, the main problem of GPR is that – unlike stake measurements, for example – it is an indirect measurement of SMB, and thus requires an interpretation which could lead to errors. Difficulties in signal processing or in signal interpretation and picking of the reflectors are the main possible sources of error.

A transmitter and receiver antenna, separated by a constant distance (common offset), are trailed behind the vehicle along the survey transect. It is usually combined with GPS measurements to obtain the geographical position. At fixed time intervals (in our case every second), the transmitting antenna emits an electromagnetic pulse, which penetrates the snow. When the electromagnetic wave reaches a layer with a different complex dielectric constant ϵ^* , it is partly reflected. This reflected signal is then received by the second antenna at the surface, and the two-way travel time (TWT) of the signal (from the surface to the interface and back) is recorded (Eisen et al., 2008). Several authors have investigated the origin of reflections in firn (e.g. Hempel et al., 2000; Eisen et al., 2003a,b; Kohler et al., 2003; Arcone et al., 2005b), but it is still unclear how continuous reflecting horizons are produced in firn and ice. In particular, “there remains some uncertainty about how the material properties in firn combine to form the continuous reflecting horizons” (Eisen et al., 2008). However, reflecting horizons have been shown by different authors and methods to be isochronous (Eisen et al., 2008 and references therein).

During the traverse, a Mal RTA (Rough Terrain Antenna) 100 MHz-frequency emitting antenna was used, with a common offset of 2 m. This frequency is a good compromise between the ideal resolution of reflecting horizons and the desired penetration depth in the firn (here at least 100 m).

The GPR produces radargrams, which are a representation of all the traces recorded along a section, with the horizontal axis representing the horizontal position and the vertical axis the two-way travel time (TWT) of the wave. Radargrams were processed with a dedicated software called ReflexWTM. Time cut, time zero correction and signal processing (gain and filters) were carried out.

Unfortunately, the quality of the radar measurements declined from 7 to 9 February 2009, probably due to a deterioration of the antenna. On 10 February, the antenna was

replaced and the resulting radargrams again became visible. But the reflectors could not be followed across this blind passage, meaning the radargrams from 7 February to the end of the transect were unusable. Consequently, we decided to analyse the profiles by starting from DC and continuing on as far as possible (i.e. until 6 February, 01:07 UTC). Table 1 summarises the radar data and Fig. 1 shows the radar section analysed.

Several steps are necessary to obtain accumulation values from a radargram:

1. The radargram requires processing to enhance the visibility of the reflecting horizons and two corrections (time zero and geometrical corrections) have to be made.
2. The vertical scale of the radargram has to be converted from time (TWT) to depth (see Sect. 2.4.2).
3. Several visible reflectors along the profile have to be selected as close as possible to dated layers of interest (i.e. volcanic or radioactive layers, see Sect. 2.3).
4. These reflectors have to be dated from firn core interpretation.
5. The snow thickness between two isochrones (or between one and the surface) has to be transformed in water equivalent depth and the latter divided by the time interval between the two isochrones (or the isochrone and the surface), as explained in Sect. 2.4.3.

A yearly averaged snow accumulation value is thus obtained.

The radar vertical resolution is given by the worst value calculated from two criteria. The first is the Rayleigh criterion (Eisen et al., 2008), which gives the resolution as one fourth of the nominal wavelength (0.75 m with a 100 MHz antenna). The second is the Ricker criterion (Eisen et al., 2008), mainly depending on the pulse length. The latter has been inferred from a later CMP measurement, and appears to be around 12 ns, which, given a velocity in the firn of $\approx 0.2 \text{ m ns}^{-1}$, finally yields an actual resolution of 1.2 m. This means that we were able to distinguish two reflectors if they were separated by a distance of at least 1.2 m.

2.2 Firn cores

Six firn cores were drilled along the transect to calibrate radar measurements with a depth–age relationship at specific points. This depth vs. age relationship is obtained by beta radioactivity measurements to detect the radioactive layers of 1955 ± 1 and 1965 ± 1 corresponding to the fallout of the atmospheric nuclear weapon tests carried out in the 1950s and 1960s (Magand, 2009). Additional deeper core data (D47 and DC) were also used for density analysis (described below in Sect. 2.4.2). Table 2 summarises the main core characteristics and the depth of the radioactive layers.

Table 1. Summary of the radar data from DC to the coast. Gaps in the data are due to technical problems encountered during the transect. The fact that data starting at 597 km from DC is unusable was due to a deterioration of the antenna, as explained in the text. See Fig. 1 for explanation of the numbering of the profiles.

Distance from DC	Date and time interval (UTC)	Comments
0 to 138 km	2009/02/02 22:58–2009/02/02 23:26	radargrams 1–6
138 to 194 km	2009/02/02 23:26–2009/02/03 05:09	no data
194 to 250 km	2009/02/03 05:09–2009/02/03 09:00	radargrams 7–8
250 to 270 km	2009/02/03 09:00–2009/02/03 22:35	no data
270 to 597 km	2009/02/03 22:35–2009/02/06 01:07	radargrams 9–17
597 to 1100 km	2009/02/06 01:07–2009/02/10 11:37	data unusable

Table 2. Firn and ice cores used in this study: name, drilling year, coordinates, altitude in m above sea level (a.s.l.), distance from DC station, total drilling depth, depth of 1955 and 1965 radioactive layers in 2009. DC data is a compilation of different datasets. The 1955 and 1965 depths at DC are based on the 2004 EPICA Dome C core depths. Corresponding depths in 2009 were estimated using stake measurements from GLACIOCLIM-SAMBA observatory, as explained in Sect. 2.5.

Name	Year	Coordinates		Altitude	Distance from DC	Total depth	1955 depth	1965 depth
		(lat. S)	(long. E)	(m.a.s.l.)	(km)	(m)	(m)	(m)
D47	1987–1989	67°23′00	138°43′00	1548	999	897	–	–
F6	2008–2009	68°44′70	134°54′53	2430	788	21	–	18–18.5
F1	2008–2009	70°08′32	134°08′01	2630	650	20.4	–	18–18.5
F2	2008–2009	71°02′50	133°01′17	2830	551	19.38	14–14.5	12–12.5
F3	2008–2009	71°56′13	131°17′42	3030	433	18.35	–	7.5–8
F4	2008–2009	72°54′17	129°10′17	3178	304	10	7–7.2	6–6.2
F5	2008–2009	73°58′27	126°34′51	3204	164	10.1	6.1–6.2	5–5.2
DC	1999–2008	75°06′00	123°21′00	3233	0	–	5.0	4.4

2.3 Selecting reflectors

Three visible reflecting horizons were selected for each profile (labeled R1 to R3). Each one was manually selected and tracked along the first profile (starting from DC) and from one profile to the next. It was possible to merge two consecutive radargrams to ensure the continuity of a reflector from one profile to the next. Depths were then calculated from the TWT, as explained below in Sect. 2.4.2. The selected reflectors are shown in Fig. 2.

Tracking the reflectors was possible until the end of radargram 17, approximately 600 km from DC (as explained above). However, tracking of reflectors R2 and R3 turned out to be difficult at the end of radargram 12 (~465 km from DC) due to very bad visibility of the radargram occurring there, and additional signal processing was applied to this radargram (dilatation and deconvolution filters) to enhance visibility. Hence, by using a deeper reflector visible before and after the blind gap as a marker, we were able to track these two horizons at the end of the profile. Nevertheless, R2 and R3 depths (and consequently accumulation) located at a distance of more than 470 km from DC remain uncertain.

2.4 Density

2.4.1 Density estimates

Density influences both the wave propagation speed in the snow and thus the conversion from TWT to depth (Sect. 2.4.2) and the final accumulation (Sect. 2.4.3). Although the influence of density on depth estimates is moderate, its impact on accumulation is more drastic. Depths of our reflectors go down to 70 m. As a result, we needed to estimate density beyond maximum depths of cores F2 to F4 (10 to 20 m). To estimate density as a function of depth and distance from DC, we thus chose to make use of two deep cores drilled at DC and D47 (Table 2). DC and D47 density measurements were fitted (third order polynomial fit) and density at each point along the transect was interpolated as a function of distance between the two sites concerned.

Figure 3 shows computed and measured density at DC, D47 and F2 to F4. Our method of fitting does not allow us to reproduce exactly the density values measured close to the surface due to extreme density variability in the top layers of snow. However, fitted values remained close to measured values in the top layers of snow (inside the measurements error bars), and reproduce measured values beyond a depth of 4 to 5 m well.

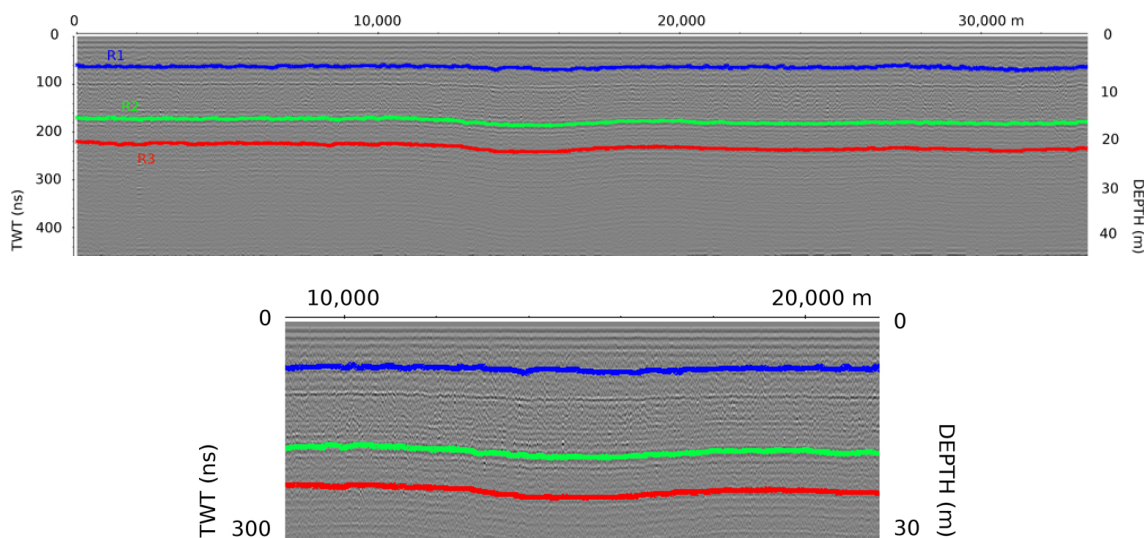


Fig. 2. Selected reflectors labeled R1 to R3 shown on radargram 5. Distance is in metres. The lower panel gives a detail of the reflectors in the middle of the radargram.

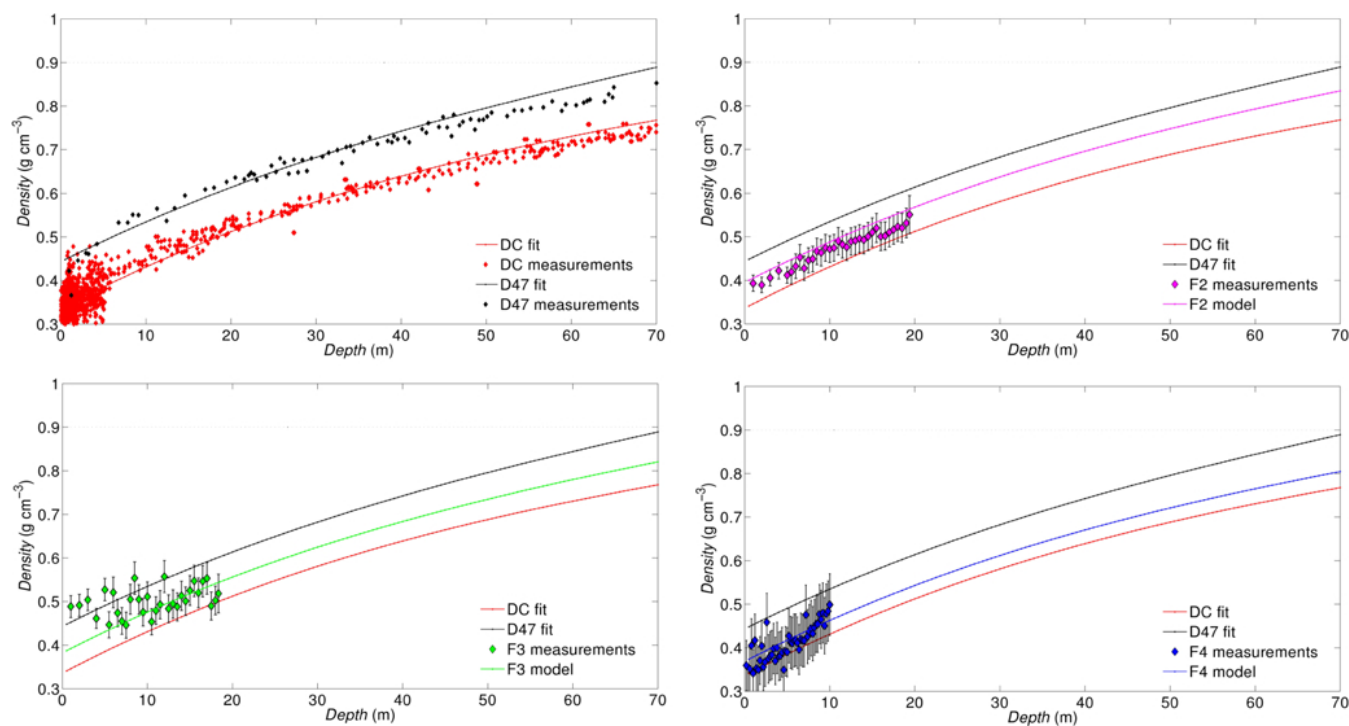


Fig. 3. Density as a function of depth. Density measurements up to 70 m in depth and their fits are represented at DC and D47 (top left panel). Measured and computed density at F2 (top right), F3 (lower left) and F4 (lower right) are also displayed. Error bars for DC and D47 measurements are not represented for reasons of clarity, but are of the same order of magnitude as for shallower cores F2 to F4 (~ 10 % error).

2.4.2 From density to wave speed and resulting conversion from TWT to depth

In order to convert TWT into depth, the knowledge of the radar wave speed is necessary. The latter is mainly controlled by snow density.

The electromagnetic wave propagation in a media is described as

$$c = c_v / \sqrt{\epsilon^*}, \quad (1)$$

where c is wave speed in the media, c_v is wave speed in the vacuum ($= 0.3 \text{ m ns}^{-1}$) and ϵ^* is complex media dielectric

constant. The latter is defined by

$$\epsilon^* = \epsilon' - i\epsilon'' \quad (2)$$

where ϵ' is the real part, called complex permittivity, which is mainly influenced by density, and ϵ'' is the imaginary part, which is mainly controlled by conductivity (Eisen et al., 2008). The imaginary part of the dielectric constant is mainly affected by the presence of liquid water (Urbini et al., 2001) and by snow chemistry. Hence, in our study, this term can be left out because the Antarctic plateau is considered to be dry and “clean”. Thus, in this case

$$\epsilon^* = \epsilon' \quad (3)$$

and, by combining Eqs. (1) and (3), we obtain

$$c = c_v / \sqrt{\epsilon'}. \quad (4)$$

Kovacs et al. (1995) proposed the following empirical approximation based on the comparison of permittivity and density measurements:

$$\epsilon' = (1 + 0.845 \times \rho)^2. \quad (5)$$

Finally, by introducing Eq. (5) into Eq. (4), we obtain the following expression:

$$c = \frac{c_v}{1 + 0.845 \times \rho}. \quad (6)$$

The latter expression was then used to determine wave speed vs. depth at the cores on the basis of density. Wave speed was then used to transform TWT into depth. A geometrical correction was necessary in the upper part of the profile to account for the fact that the emitter and receiver antennas were separated by a common-offset of 2 m.

Different sources of error can affect depth estimates, mainly wave speed estimates (density uncertainties, firm depth correction), time-zero correction and selection of the reflectors. Considering these error sources, we estimated a depth uncertainty of about 1 m.

2.4.3 From density to accumulation

Density values were used to transform accumulation in centimetres of snow into accumulation in cm water equivalent (w.e.) as follows:

$$a = \int_{z_{n-1}}^{z_n} \frac{s \times \rho(z)}{z_n - z_{n-1}} dz \quad (7)$$

where n is the number of the reflector concerned R , z is depth, s is accumulation in cm of snow, a is accumulation in cm w.e., and ρ is density.

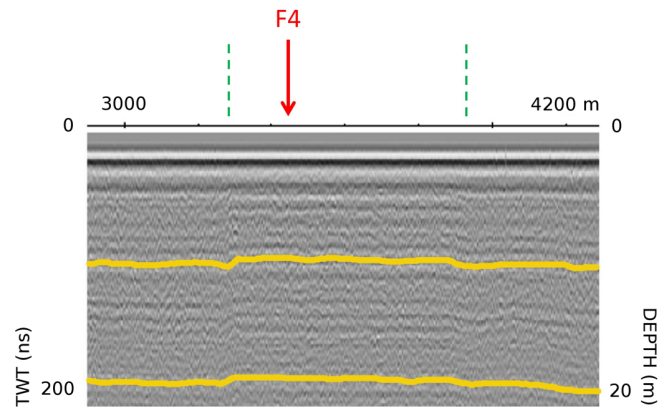


Fig. 4. Transition between the “real” and “natural” snow surface visible on radargram 9 in the vicinity of core F4. The first dotted line corresponds to the point where the radar vehicle left the transect route and the second one to the point where it got back on the route.

2.5 Dating reflectors

Dating of the selected reflectors by direct interpolation between two layers of known age at DC was not possible. Indeed, the snow surface in the vicinity of the station as well as on the transect route is constantly modified by the passage of vehicles and maintenance work, and so the “real” surface does not correspond to what would have been the “natural” undisturbed surface in 2009. Depths measured using radar thus refer to the disturbed real surface and not to the natural one, hence preventing the simple dating of the reflectors. The surface was intact only in the vicinity of firm core sites and, as the radar vehicle had to leave the transect route to get close to those sites, the surface displayed on the radargrams is natural for only a short distance. This is clearly visible on the radargram close to the F4 firm core (Fig. 4). Consequently, to date the reflectors, we had to use in a complementary way the F4 site where the surface was natural and the DC core where some layers are well dated.

At DC, as explained above, the absolute depths of the selected reflectors are not correct but the depth intervals between reflectors (R1–R2 and R2–R3) make sense. Besides, well dated volcanic layers (Table 3) in the 2004 EPICA Dome C ice core provide a depth–age scale at DC. Depths were determined for 2004, the year the EPICA ice core was drilled. Then data from GLACIOCLIM-SAMBA observatory stakes measurements¹ at DC were used to account for the 43 cm of snow that accumulated between 2004 and 2009. Knowing the depth–age relationship at DC (Fig. 5), it was possible to calculate the age interval between the reflectors. As the curve is non-linear, the uncertainty in the absolute depths led to uncertainty in the age interval but the error was only small, i.e. an error of 1 m in the location of the reflectors led to a 3 % difference in the age intervals. We then obtained

¹Website: <http://www-1gge.ujf-grenoble.fr/ServiceObs/SiteWebAntarc/dc.php>

Table 3. Characteristic volcanic layers in the EPICA Dome C core: name, age, depth at DC in 2004 (adapted from Castellano et al., 2005) and estimated depth at DC in 2009 (for an undisturbed surface).

Name of layer	Age	Depth at DC in 2004 (m)	Estim. depth at DC in 2009 (m)
Agung	1964 ± 1	3.9	4.4
Tambora	1816 ± 4	12.5	12.9
Jorullo-Taal	1758 ± 6	15.36	15.8
Serua	1696 ± 4	18.62	19.05

a time interval of 142 ± 4 yr between reflectors R1 and R2, and of 69 ± 2 yr between R2 and R3.

At F4, a 10 m core was drilled, and the 1955 and 1965 radioactive horizons were identified. The density profile was measured and the 2009–1955 snow accumulation then computed (Table 4). The R1, R2 and R3 depths were obtained from radargrams and the R1–R2 and R2–R3 snow accumulation rate in cm a⁻¹ (Table 4) was calculated.

The 1955–R1 snow accumulation rate at F4 was not known a priori, but was interpolated between the 1955–2009 (15.0 cm snow a⁻¹) and the R1–R2 (11.7 cm snow a⁻¹) rates, which makes sense because the values are relatively close. From this snow accumulation rate, we obtained the R1–1955 time interval and, finally, the age of the R1, R2, R3 layers, respectively 1941 ± 1, 1799 ± 5 and 1730 ± 7 AD.

3 Results

3.1 Undulating structures

The East Antarctic plateau is usually considered to be flat up to the break in slope, which, in the study’s area, is located ~ 230 km from the coast (i.e. 870 km from DC), and accumulation is assumed almost uniform up to that point (Pettré et al., 1986). However, GPS data (Fig. 6) revealed that there is a first change in slope around 300 km from DC. Radargrams then showed some undulating structures located between 300 and 600 km from DC (Fig. 7). In the middle of the plateau, 10 km wavelength undulations appeared with vertical amplitudes ranging from 5 to 20 m (Fig. 7), which seemed to be amplified with depth. These structures are also visible in Fig. 6, which illustrates changes in the surface elevation and in depth of the reflectors with increasing distance from DC.

3.2 Snow accumulation

Snow accumulation between DC and a point at 600 km from DC was plotted against core data and accumulation values from previous studies (Fig. 8) and model results (Fig. 9). Only our 1730–1799 and 1799–1941 values are shown, along

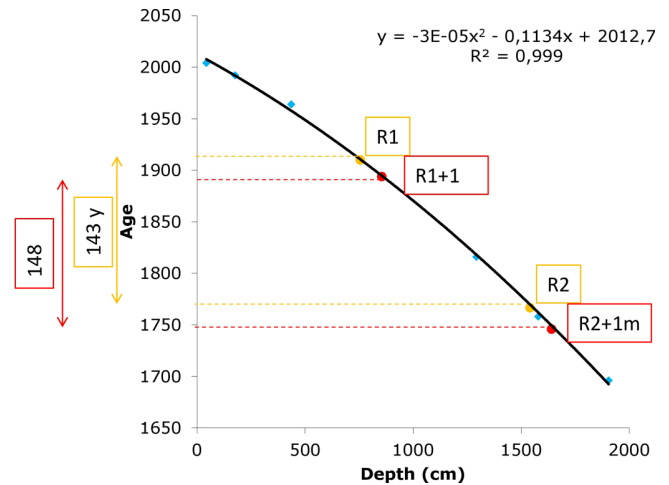


Fig. 5. 2009 Depth–age relationship at DC (black curve) based on dating of EPICA Dome C volcanic layers (blue dots). The age interval between reflectors R1 and R2 is shown, as well as the age interval between those two reflectors if a 1 m-shift in depth is applied.

with core values for the period 1965–2009. Radar values for 1941–2009 were left out because the surface of the transect route is no longer “natural” (Sect. 2.5), leading to a greater margin of error for reflectors close to the surface. For example, on the transect route close to core F4, a surface-induced accumulation error of ~ +11 % was estimated for the period 1941–2009, while the error was less than +5 % and +3 % for 1799–1941 and 1730–1799 periods, respectively. We consequently decided not to take the 1941–2009 accumulation values into consideration.

It should be noted that the accumulation ratio (in cm of snow, not shown) between 1965–2009 core estimates and 1730–1799 or 1799–1941 radar estimates was almost the same from DC to around 450 km from DC, but was greater at F2. For example, calculating the ratio $(a_1 - a_3)/a_1$ between 1965–2009 (a_1) and 1730–1799 (a_3) time periods yielded values of 0.22 to 0.27 for DC to F3, while the F2 value was 0.36. This could indicate an error in the selection of the reflectors at distances of more than 470 km from DC, as explained in Sect. 2.3. Accumulation estimates beyond this point should thus be considered with caution.

Accumulation data were compared to four SMB climatologies (Fig. 9):

- We first compared our results to those of Arthern et al. (2006) and van de Berg et al. (2006), which are currently assumed to be among the most reliable estimates of broad-scale patterns of SMB across Antarctica. The results of Arthern et al. (2006) were obtained by continuous-part universal kriging of SMB field measurements over the period 1950–1990 (Vaughan and Russell, 1997) with a background model based on passive microwaves data, whereas the SMB values of

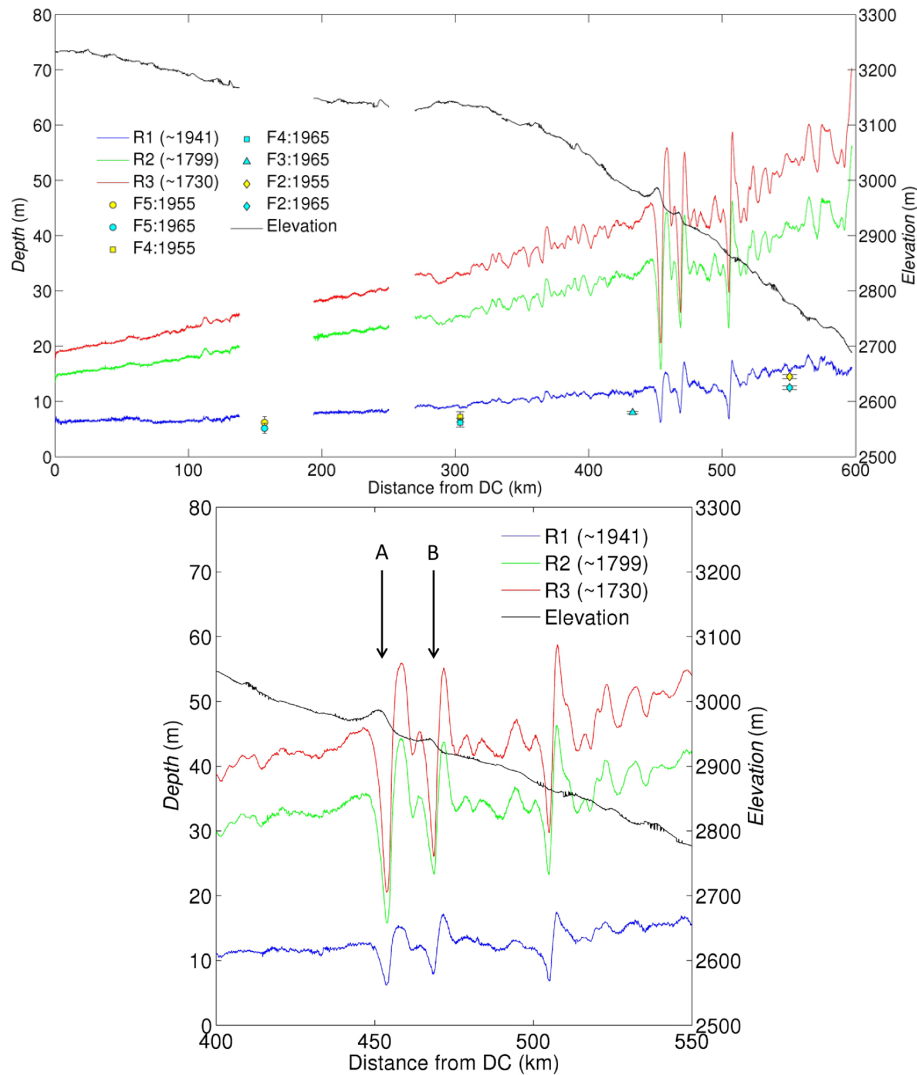


Fig. 6. Depth of reflectors and surface elevation vs. distance from DC. Coloured symbols represent depths of the 1955 and 1965 layers measured on the cores for the purpose of comparison, and their associated error bars. The lower panel focuses on undulations located between 400 and 550 km from DC, with A and B referring to two local elevation peaks that link with undulations, as discussed in the text.

Table 4. Summary of the parameters which were measured or computed at F4 to calculate ages, and ensuing computed age for each reflector.

Layers	Intervals	Measured depth (cm)	Depth interval (cm)	Snow accu (cm a ⁻¹)	Time interval (yr)	Computed age
1955	1955–2009		700–720	15.00 (measured)	54	
	R1–1955	700–720				
R1		893	173–193	13.33 (interpolated)	14 ± 1 (computed)	1941 ± 1
R2		2548	1655	11.65 (measured)	142 ± 4 (from DC core)	1799 ± 5
R3		3294	746	10.82 (measured)	69 ± 2 (from DC core)	1730 ± 7

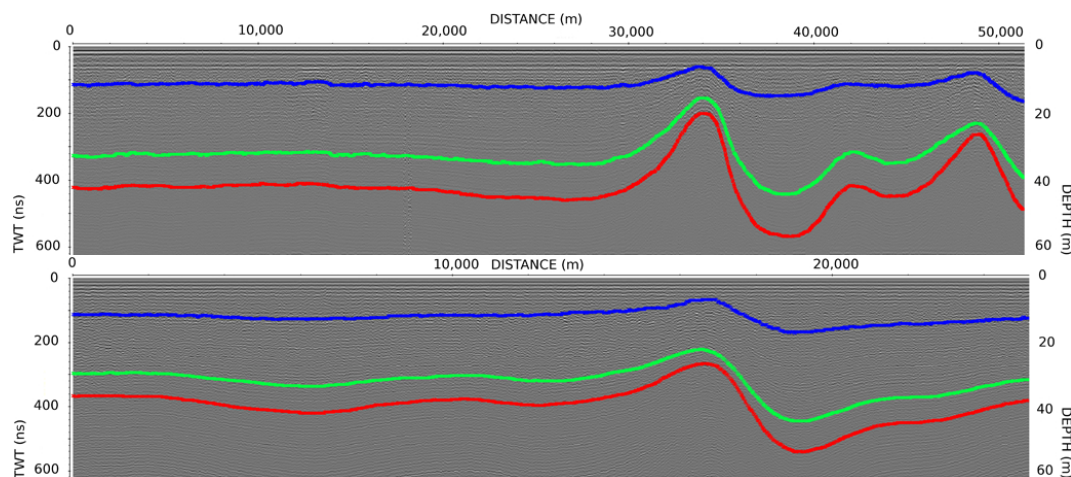


Fig. 7. Undulating structures visible on radargram 12 (4 February, 22:35 UTC to 5 February, 02:09 UTC, between 450 and 470 km from DC) and radargram 14 (5 February, 04:41 UTC to 06:39 UTC, between 495 and 510 km from DC).

van de Berg et al. (2006) were the results of the Regional Atmospheric Climate Model v.2 (RACMO2), which were calibrated with SMB field observations from the database of Vaughan and Russell (1997). In the latter model, RACMO2 was run at a resolution of 55 km without snowdrift with lateral boundary conditions from ERA-40 (Uppala et al., 2005) for the period 1980 to 2004.

- We also compared our SMB data to ERA-Interim values. ERA-Interim is the most recent reanalysis (Simmons et al., 2006) from the European Centre for Medium-Range Weather Forecasts (ECMWF), and covers the period 1989 to present. A reanalysis is the result of complex data assimilation to produce an optimal combination of observations and meteorological model results. The main advances of ERA-Interim over ERA-40 are a finer spectral truncation, improved model physics and a more efficient data assimilation system.
- Finally we compared our results to the SMB produced from an atmospheric global circulation model, LMDZ4 (Hourdin et al., 2006), which is the atmospheric component of the IPSL-CM4 climate system model (Marti et al., 2006) that participated in the World Climate Research Programme's Coupled Model Inter-Comparison Project phase 3 (CMIP3) exercise to build the IPCC 4th assessment report (Meehl et al., 2007). The model used in the present study includes several improvements for the simulation of polar climates suggested by Krinner et al. (1997).

4 Discussion

4.1 Undulating structures

The undulating structures visible in Figs. 6 and 7 are probably caused by redistribution of snow by the wind due to gravity waves that are triggered at breaks in a slope (Gallée and Pettré, 1998). This phenomenon was described in Adelie Land coastal areas by Pettré et al. (1986), where 40 km wavelength isochronal undulations were observed below the break point at 230 km from the coast. However, Pettré et al. (1986) did not find undulations further inland, and suggested that accumulation on the plateau was relatively uniform. However, it should be noted that their observations result from a 10 km spaced stake network until 430 km from the coast (670 km from DC), and three core measurements between DC and 670 km from DC. Consequently, they were not able to capture structures with wavelengths of around 10 km like the ones visible on our radargrams. As noted earlier, another break in the slope is also visible around 300 km from DC (Fig. 6). It is interesting to note that, like in Pettré's study, the undulations start just after that break in slope.

The undulations' link with local topography is clearly visible in Figs. 6, 8 and 9. Low accumulation intervals between 450 and 470 km from DC are located in the lee of local elevation peaks (labelled A and B in Fig. 6), where the surface slope is the steepest, reflecting local strong ablation conditions due to high snow erosion rates caused by divergence in the katabatic wind field (e.g. van den Broeke et al., 2006; Favier et al., 2011). The crest of deep undulations is located downwind from the surface crest, where the slope is closer to zero. Regarding undulations variations with time, the progressive steepening of fold limbs visible in Fig. 7 is a well-known feature caused by spatial variations in accumulation rates (see e.g. Arcone et al., 2005b).

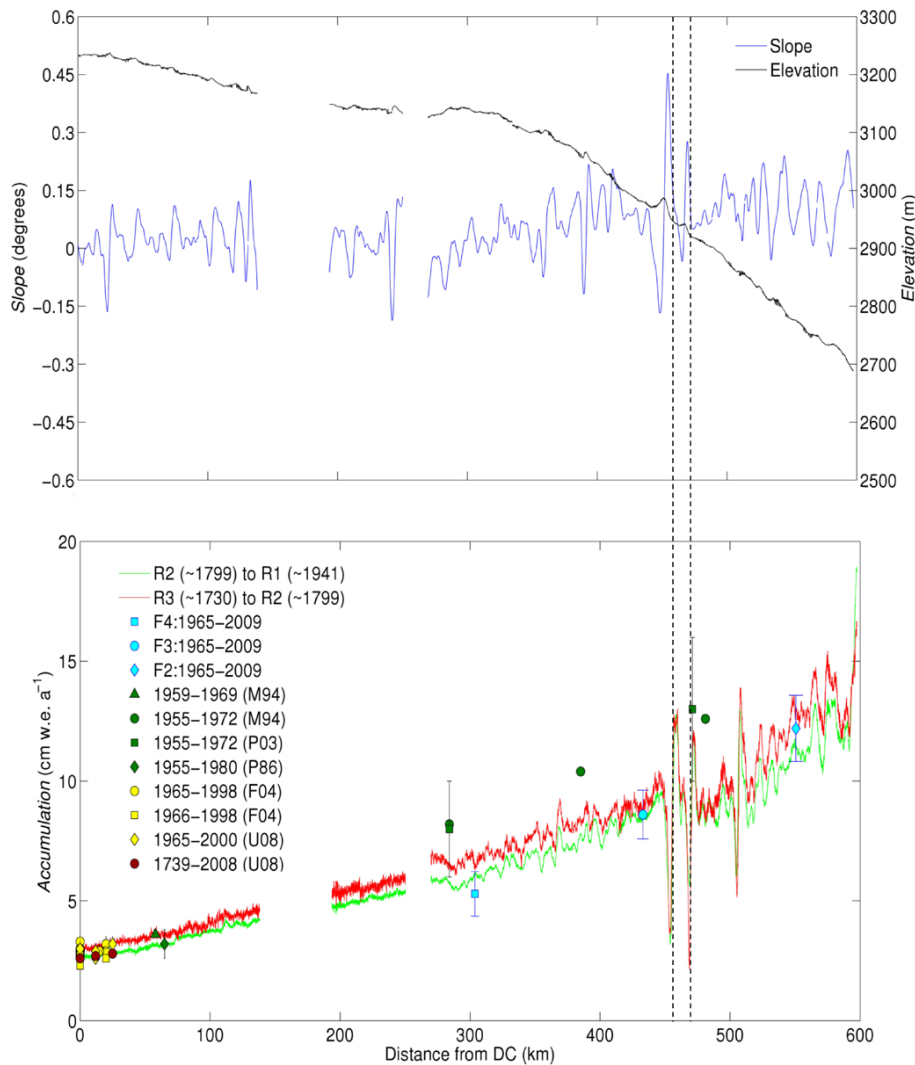


Fig. 8. Comparison of our accumulation results (radar and core measurements) and of previous studies along the transect. M94 = Mulvaney et al. (1994); P03 = Pourchet et al. (2003); P86 = Pettré et al. (1986); F04 = Frezzotti et al. (2004); U08 = Urbini et al. (2008). Upper panel shows elevation and slope.

To conclude, the undulations we observe would be the result of accumulation variations caused by interactions between katabatic wind and local topography. These processes are described in Arcone et al. (2005b).

4.2 Spatial variations in accumulation

A gradual increase in accumulation from DC to the end of the transect was observed (Figs. 8 and 9). This is consistent with previous observations in the region (see e.g. Pourchet et al., 1983; Pettré et al., 1986) along with a gradual increase in humidity from DC to the coast (Bromwich et al., 2004). Moreover, major variations in accumulation are reflected by the undulating structures described above (Figs. 8 and 9).

Radar and core accumulation values matched most historical measurements (Fig. 8), although the time periods studied were not the same. Several observations can be made:

- Our radar accumulation results agree fairly well with measurements made within 25 km of DC by Frezzotti et al. (2004) and Urbini et al. (2008) for the period 1965–“recent”, and with estimates made by Urbini et al. (2008) for the period 1739–2008. Differences remained within less than 1 cm w.e. a^{-1} , i.e. less than 25%. Changes in accumulation in the past 20 yr observed by Urbini et al. (2008) could not be checked here as radar data only allow estimations for older periods.
- Accumulation estimates made for the period 1955–1972 by Mulvaney and Wolff (1994) and Pourchet et al. (2003) are systematically higher than our radar and core

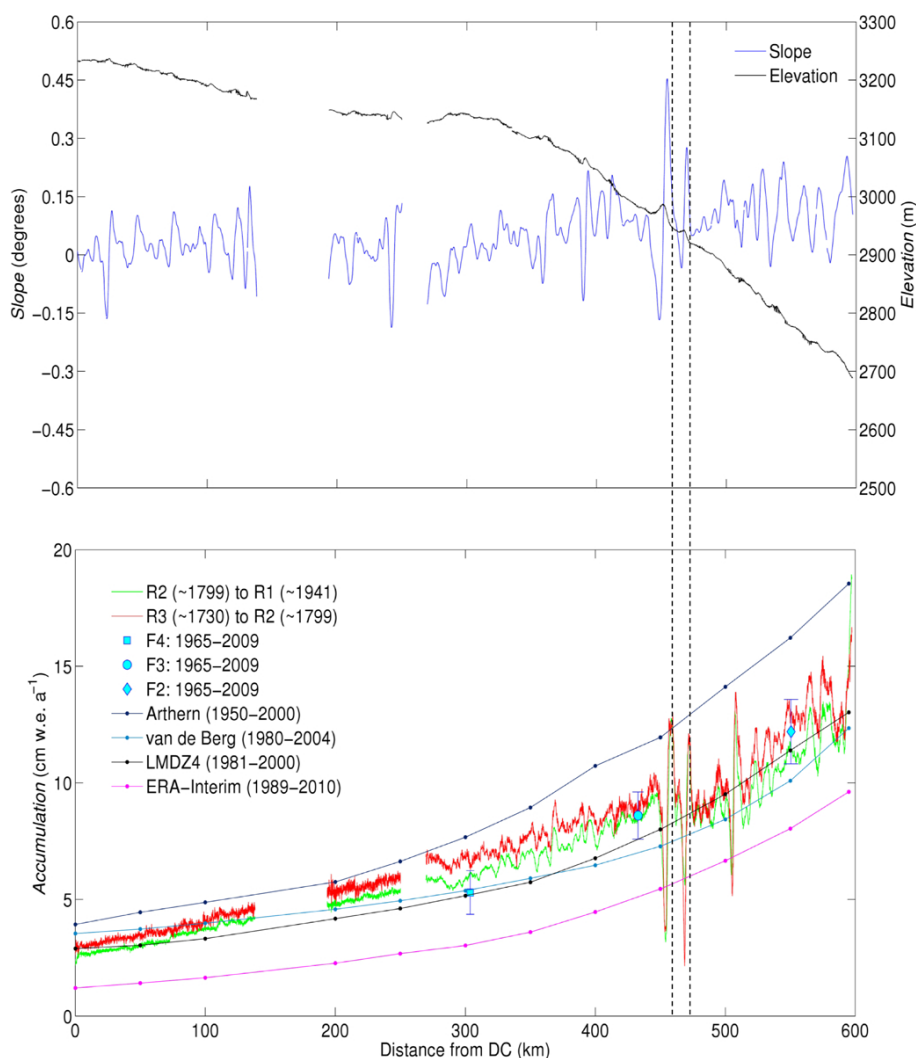


Fig. 9. Comparison of our accumulation results (radar and core measurements) and modelling results along the transect. Upper panel shows elevation and slope.

estimates. On the contrary, estimates by Mulvaney and Wolff (1994) and Petré et al. (1986) for the periods 1959–1969 and 1955–1980, respectively, are in good agreement with our results. In addition, Agosta et al. (2011) found little change in coastal SMB after the 1970s. This could lead to the conclusion that 1955–1972 was an abnormally wet period compared to the last centuries, although this conclusion should be considered with caution because of the uncertainties linked to historical data for the period 1955–1972 and our estimates. Further analysis of this particular period would be required.

Regarding model validation, all four SMB climatologies are close to our accumulation results (Fig. 9). However, some differences between models can be noted:

- Accumulation modelled by Arthern is systematically higher than our results, indicating a wetter modelled climate. This is probably due to the fact that Arthern’s accumulation map is based on available accumulation measurements. Between 200 and 500 km from DC, these correspond to data from Mulvaney and Wolff (1994) and Pourchet et al. (2003), which display higher accumulation values than our own (Fig. 8). Moreover, Pourchet’s measurement made around 470 km from DC could have been made on one of the undulations described earlier.
- ERA-INTERIM reanalysis, on the contrary, yield much drier results than our own. This situation contrasts with the coastal area of Adelie Land where data of Agosta et al. (2011) were in good agreement with ERA-Interim results, whereas ERA-40 yields slightly too humid values due to larger sublimation

in ERA-Interim. Nevertheless, our conclusions confirm that ERA-Interim generally yield too dry values over plateaus, as observed by Agosta (2012). This is also the reason why ERA-40 SMB integrated over the whole of Antarctica represents the lower limit of SMB values in the literature (e.g. Monaghan et al., 2006b).

- van de Berg model results are in good agreement with our accumulation estimates. Their climatology is refitted by altitude intervals on Vaughan and Russell (1997) data, thus it does not correspond to kriging. As a result, unlike Arthern et al. (2006), their method does not introduce local biases due to old measurements made in our study region. This points to the biases introduced by doubtful measurements in SMB extra- and interpolations, and confirms the need for data quality control, such as proposed by Magand et al. (2007).
- The LMDZ4 model is “free from any meteorological observational constraint” (Agosta et al., 2011). However, it is the model which agrees the best with our accumulation values, remaining within the margin of uncertainty of our 1965–2009 core estimates. It reacts particularly well in the study region, as observed previously in the coastal area (Agosta et al., 2011). This is surprising because “models that use observed sea ice, such as ERA, are expected to do better in depicting the absolute amount of precipitation than climatic models, since precipitation and evaporation rates depend on the extent of sea ice” (Agosta et al., 2011).

4.3 Temporal variations in accumulation

Temporal variations should be interpreted with caution. Indeed, density is used to convert accumulation in cm into cm w.e. (as explained in Sect. 2.4.3). Accumulation in cm of snow (not shown) and in cm w.e. (Figs. 8 and 9) evolve very differently with time due to snow densification. Considering the uncertainty margin on our accumulation results (which can be considered at least equal to uncertainties in core estimates, i.e. 11 to 17%), accumulation in cm w.e. did not significantly increase with time. Indeed, if (1) dating of layers at DC based on the EPICA Dome C ice core and (2) our density estimates are valid, there was no difference in accumulation between the three study periods (radar 1730–1799, radar 1799–1941 and firn cores 1965–2009). However, because of the difficulty involved in estimating density, it is risky to draw conclusions variability of accumulation with time.

5 Conclusions and outlook

A radar transect was conducted in Adelie Land (East Antarctica) in 2008–2009, between DC station and the coast and six

complementary firn cores were drilled. This long continuous radar dataset is one of the few obtained in the region.

Study of the 600 km-long usable dataset yielded three major results:

1. Accumulation increases gradually with an increase in the distance from DC, which is consistent with findings from previous studies in this region. Regarding spatial variations in accumulation, historical accumulation data and results from modelling studies along the transect are in good agreement with our results.
2. Previously undocumented 10 km wavelength undulations exist in a region located between 300 and 600 km from DC. These require further analyses in future studies, notably via atmospheric modelling (MAR model, Gallée and Schayes, 1994), assuming that the model can capture such a fine resolution. It also provides information that is useful for the search of new drilling sites. We now know that the section from 450 to 500 km from DC would not be suitable for drilling a new core because of the high variability of accumulation.
3. There is no significant change in accumulation with time, if dating of layers at DC based on the EPICA Dome C ice core and our density estimates are considered valid. Indeed, accumulation results rely heavily on density estimates, and consequently, drawing conclusions regarding changes in accumulation with time is difficult. Density is only measured occasionally and measurements are often not deep enough. We took advantage of two deep cores drilled at DC and D47 (1000 km apart) to estimate density along the transect, as an interpolation in function of the distance to those two sites.

In the long term, a more rapid method of measuring density is needed to ensure more frequent density measurements. This would be useful for all studies that require accurate density estimates.

New radar and firn core measurements were obtained during a transect between DC and Vostok stations in 2011–2012. Upcoming analysis of these new data should provide complementary knowledge about East-Antarctic SMB.

Acknowledgements. We would like to thank M. Frezzotti, and S. Urbini for the advice they gave at the start of this study. We also thank Cécile Agosta for her help with model accumulation results, the GLACIOCLIM-SAMBA observatory for providing stake data at DC, and Paul Duval and Hubert Gallée for the advice they gave on specific topics related to this study. This study was made possible thanks to IPEV and ANR funding (“VANISH” project no. ANR-07-VULN-013 and “Dome A” project no. ANR-07-BLAN-0125).

Edited by: M. Schneebeli



The publication of this article is financed by CNRS-INSU.

References

- Agosta, C., Favier, V., Genthon, C., Gallée, H., Krinner, G., Lenaerts, J., and van den Broeke, M.: A 40-year accumulation dataset for Adelie Land, Antarctica and its application for model validation, *Clim. Dynam.*, 38, 75–86, doi:10.1007/s00382-011-1103-4, 2011.
- Agosta, C.: Evolution du bilan de masse de surface Antarctique par régionalisation physique et conséquences sur les variations du niveau des mers, Ph.D. thesis, Université Joseph Fourier, Grenoble, 2012.
- Arcone, S., Spikes, V., and Hamilton, G.: Phase structure of radar stratigraphic horizons within Antarctic firn, *Ann. Glaciol.*, 41, 10–16, 2005a.
- Arcone, S., Spikes, V., and Hamilton, G.: Stratigraphic variation within polar firn caused by differential accumulation and ice flow: interpretation of a 400 MHz short-pulse radar profile from West Antarctica, *J. Glaciol.*, 51, 407–422, 2005b.
- Arthern, R., Winebrenner, D., and Vaughan, D.: Antarctic snow accumulation mapped using polarization of 4.3-cm wavelength microwave emission, *J. Geophys. Res.*, 111, D06107, doi:10.1029/2004JD005667, 2006.
- Bromwich, D., Guo, Z., Bai, L., and Chen, Q.: Modeled antarctic precipitation. Part I: Spatial and temporal variability, *J. Climate*, 17, 427–447, 2004.
- Castellano, E., Becagli, S., Hansson, M., Hutterli, M., Petit, J. R., Rampino, M. R., Severi, M., Steffensen, J. P., Traversi, R., and Udisti, R.: Holocene volcanic history as recorded in the sulfate stratigraphy of the European Project for Ice Coring in Antarctica Dome C (EDC96) ice core, *J. Geophys. Res.*, 110, D06114, doi:10.1029/2004JD005259, 2005.
- Daniels, J.: Ground Penetrating Radar Fundamentals, prepared as an appendix to a report to the US EPA, Region V, Department of Geological Sciences, The Ohio State University, 2000.
- Eisen, O., Wilhelms, F., Nixdorf, U., and Miller, H.: Identifying isochrones in GPR profiles from DEP-based forward modeling, *Ann. Glaciol.*, 37, 344–350, 2003a.
- Eisen, O., Wilhelms, F., Nixdorf, U., and Miller, H.: Revealing the nature of radar reflections in ice: DEP-based FDTD forward modeling, *Geophys. Res. Lett.*, 30, 1218, doi:10.1029/2002GL016403, 2003b.
- Eisen, O., Frezzotti, M., Genthon, C., Isaksson, E., Magand, O., Broeke, M., Dixon, D., Ekaykin, A., Holmlund, P., Kameda, T., Karlöf, L., Kaspari, S., Lipenkov, V., Oerter, H., Takahashi, S., and Vaughan, D.: Ground-based measurements of spatial and temporal variability of snow accumulation in East Antarctica, *Rev. Geophys.*, 46, RG2001, doi:10.1029/2006RG000218, 2008.
- Favier, V., Agosta, C., Genthon, C., Arnaud, L., Trouvillez, A., and Gallée, H.: Modeling the mass and surface heat budgets in a coastal blue ice area of Adelie Land, Antarctica, *J. Geophys. Res.*, 116, F03017, doi:10.1029/2010JF001939, 2011.
- Frezzotti, M., Pourchet, M., Flora, O., Gandolfi, S., Gay, M., Urbini, S., Vincent, C., Becagli, S., Gragnani, R., Proposito, M., Severi, M., Traversi, R., Udisti, R., and Fily, M.: New estimations of precipitation and surface sublimation in East Antarctica from snow accumulation measurements, *Clim. Dynam.*, 23, 803–813, 2004.
- Frezzotti, M., Pourchet, M., Flora, O., Gandolfi, S., Gay, M., Urbini, S., Vincent, C., Becagli, S., Gragnani, R., Proposito, M., Severi, M., Traversi, R., Udisti, R., and Fily, M.: Spatial and temporal variability of snow accumulation in East Antarctica from traverse data, *J. Glaciol.*, 51, 113–124, 2005.
- Gallée, H. and Pettré, P.: Dynamical constraints on katabatic wind cessation in Adélie Land, Antarctica, *J. Atmos. Sci.*, 55, 1755–1770, 1998.
- Gallée, H. and Schayes, G.: Development of a 3-dimensional meso-gamma primitive equation model – katabatic winds simulation in the area of terra-nova bay, Antarctica, *Mon. Weather Rev.*, 122, 671–685, 1994.
- Genthon, C., Lardeux, P., and Krinner, G.: The surface accumulation and ablation of a blue ice area near Cap Prudhomme, Adélie Land, Antarctica, *J. Glaciol.*, 53, 635–645, 2007.
- Helsen, M., van den Broeke, van de Wal, R., van de Berg, W., van Meijgaard, E., Davis, C., Li, Y., and Goodwin, I.: Elevation changes in Antarctica mainly determined by accumulation variability, *Science*, 320, 1626–1629, 2008.
- Hempel, L., Thyssen, F., Gundestrup, N., Clausen, H., and Miller, H.: A comparison of radio-echo sounding data and electrical conductivity of the GRIP ice core, *J. Glaciol.*, 46, 369–374, 2000.
- Hourdin, F., Musat, I., Bony, S., Braconnot, P., Codron, F., Dufresne, J.-L., Fairhead, L., Filiberti, M.-A., Friedlingstein, P., Grandpeix, J.-Y., Krinner, G., LeVan, P., Li, Z.-X., and Lott, F.: The LMDZ4 general circulation model: climate performance and sensitivity to parametrized physics with emphasis on tropical convection, *Clim. Dynam.*, 27, 787–813, 2006.
- Kohler, J., Moore, J., and Isaksson, E.: Comparison of modelled and observed responses of a glacier snowpack to ground-penetrating radar, *Ann. Glaciol.*, 37, 293–297, 2003.
- Kovacs, A., Gow, A., and Morey, R.: The in-situ dielectric constant of polar firn revisited, *Cold Reg. Sci. Technol.*, 23, 245–256, 1995.
- Krinner, G., Genthon, C., Li, Z., and Le Van, P.: Studies of the Antarctic climate with a stretched-grid general circulation model, *J. Geophys. Res.*, 102, 13731–13745, 1997.
- Magand, O.: Bilan de masse de surface Antarctique: techniques de mesure et analyse critique, Ph.D. thesis, Université Joseph Fourier, Grenoble, 2009.
- Magand, O., Frezzotti, M., Pourchet, M., Stenni, B., Genoni, L., and Fily, M.: Climate variability along latitudinal and longitudinal transects in East Antarctica, *Ann. Glaciol.*, 39, 351–358, 2004.
- Magand, O., Genthon, C., Fily, M., Krinner, G., Picard, G., Frezzotti, M., and Ekaykin, A.: An up-to-date quality-controlled surface mass balance data set for the 90°–180° E Antarctica sector and 1950–2005 period, *J. Geophys. Res.*, 112, D12106, doi:10.1029/2006JD007691, 2007.
- Marti, O., Braconnot, P., Bellier, J., Benschila, R., Bony, S., Brockmann, P., Cadule, P., Caubel, A., Denvil, S., Dufresne,

- J.-L., Fairhead, L., Filiberti M.-A., Fichetef, T., Foujols, M.-A., Friedlingstein, P., Grandpeix, J.-Y., Hourdin, F., Krinner, G., Lévy, C., Madec, G., Musat, I., De Noblet, N., Polcher, J., and Talandier, C.: The new IPSL climate system model: IPSL-CM4, Note du Pôle de Modélisation 26, ISSN 1288-1619, 88 pp., 2006.
- Meehl, G., Stocker, T., Collins, W., Friedlingstein, A., Gaye, A., Gregory, J., Kitoh, A., Knutti, R., Murphy, J., Noda, A., Raper, S. C. B., Watterson, I. G., Weaver, A. J., and Zhao, Z.-C.: Global climate projections, in: *Climate Change 2007: The Physical Science Basis. Contribution of Working Group I to the Fourth Assessment Report of the Intergovernmental Panel on Climate Change*, edited by: Solomon, S., Qin, D., Manning, M., Chen, Z., Marquis, M., Averyt, K., Tignor, M., and Miller, H., Cambridge University Press, 2007.
- Monaghan, A., Bromwich, D., Fogt, R., Wang, S., Mayewski, P., Dixon, D., Ekaykin, A., Frezzotti, M., Goodwin, I., Isaksson, E., Kaspari, S., Morgan, V., Oerter, H., Van Ommen, T., Van der Veen, C., and Wen, J.: Insignificant change in Antarctic snowfall since the International Geophysical Year, *Science*, 313, 827–831, doi:10.1126/science.1128243, 2006a.
- Monaghan, A., Bromwich, D., and Wang, S.: Recent trends in Antarctic snow accumulation from Polar MM5 simulations, *Philos. T. R. Soc. A*, 364, 1683–1708, 2006b.
- Muller, K., Sinisalo, A., Anschutz, H., Hamran, S., Hagen, J., McConnell, J., and Pasteris, D.: An 860 km surface mass-balance profile on the East Antarctic plateau derived by GPR, *Ann. Glaciol.*, 51, 1–8, 2010.
- Mulvaney, R. and Wolff, E.: Spatial variability of the major chemistry of the Antarctic ice sheet, *Ann. Glaciol.*, 20, 440–447, 1994.
- Petit, J., Jouzel, J., Pourchet, M., and Merlivat, L.: A detailed study of snow accumulation and stable isotope content in Dome C (Antarctica), *J. Geophys. Res.*, 87, 4301–4308, 1982.
- Pettré, P., Pinglot, J., Pourchet, M., and Reynaud, L.: Accumulation distribution in Terre Adélie, Antarctica: effect of meteorological parameters, *J. Glaciol.*, 32, 486–500, 1986.
- Pourchet, M., Pinglot, F., and Lorius, C.: Some meteorological applications of radioactive fallout measurements in Antarctic snows, *J. Geophys. Res.*, 88, 6013–6020, 1983.
- Pourchet, M., Magand, O., Frezzotti, M., Ekaykin, A., and Winther, J.: Radionuclides deposition over Antarctica, *J. Environ. Radioactiv.*, 68, 137–158, 2003.
- Richardson, C. and Holmlund, P.: Spatial variability at shallow snow-layer depths in central Dronning Maud Land, East Antarctica, *Ann. Glaciol.*, 29, 10–16, 1999.
- Richardson, C., Aarholt, E., Hamran, S., Holmlund, P., and Isaksson, E.: Spatial distribution of snow in western Dronning Maud Land, East Antarctica, mapped by a ground-based snow radar, *J. Geophys. Res.*, 102, 20343–20353, 1997.
- Simmons, A., Uppala, S., Dee, D., and Kobayashi, S.: ERA-Interim: new ECMWF reanalysis products from 1989 onwards, *ECMWF Newsl.*, 110, 25–35, 2006.
- Solomon, S., Qin, D., Manning, M., Chen, Z., Marquis, M., Averyt, K., Tignor, M., and Miller, H.: *IPCC, 2007: Climate Change 2007: The Physical Science Basis. Contribution of Working Group I to the Fourth Assessment Report of the Intergovernmental Panel on Climate Change*, 2007.
- Uppala, S., Kallberg, P., Simmons, A., and collaborators: The ERA-40 re-analysis, *Q. J. Roy. Meteor. Soc.*, 131, 2961–3012, 2005.
- Urbini, S., Vittuari, L., and Gandolfi, S. A.: GPR and GPS data integration: examples of application in Antarctica, *Ann. Geofis.*, 44, 687–702, 2001.
- Urbini, S., Frezzotti, M., Gandolfi, S., Vincent, C., Scarchilli, C., Vittuari, L., and Fily, M.: Historical behaviour of Dome C and Talos Dome (East Antarctica) as investigated by snow accumulation and ice velocity measurements, *Global Planet. Change*, 60, 576–588, 2008.
- van de Berg, W., van den Broeke, M., Reijmer, C., and van Meijgaard, E.: Reassessment of the Antarctic surface mass balance using calibrated output of a regional atmospheric climate model, *J. Geophys. Res.*, 111, D11104, doi:10.1029/2005JD006495, 2006.
- van den Broeke, M., van de Berg, W. J., van Meijgaard, E., and Reijmer, C.: Identification of Antarctic ablation areas using a regional climate model, *J. Geophys. Res.*, 111, D18110, doi:10.1029/2006JD007127, 2006.
- Vaughan, D. and Russell, J.: *Compilation of Surface Mass Balance Measurements in Antarctica*, Internal Rep. ES4/8/1/1997/1, British Antarctic Survey, Cambridge, UK, 1997.